



---

**LES Modeling of Non-local effects using Statistical Coarse-graining**

**Karthik Duraisamy**  
**REGENTS OF THE UNIVERSITY OF MICHIGAN**

---

**12/12/2019**  
**Final Report**

**DISTRIBUTION A: Distribution approved for public release.**

**Air Force Research Laboratory**  
**AF Office Of Scientific Research (AFOSR)/ RTA2**  
**Arlington, Virginia 22203**  
**Air Force Materiel Command**

DISTRIBUTION A: Distribution approved for public release

<b>REPORT DOCUMENTATION PAGE</b>		<i>Form Approved</i> <i>OMB No. 0704-0188</i>	
<p>The public reporting burden for this collection of information is estimated to average 1 hour per response, including the time for reviewing instructions, searching existing data sources, gathering and maintaining the data needed, and completing and reviewing the collection of information. Send comments regarding this burden estimate or any other aspect of this collection of information, including suggestions for reducing the burden, to Department of Defense, Executive Services, Directorate (0704-0188). Respondents should be aware that notwithstanding any other provision of law, no person shall be subject to any penalty for failing to comply with a collection of information if it does not display a currently valid OMB control number.</p> <p><b>PLEASE DO NOT RETURN YOUR FORM TO THE ABOVE ORGANIZATION.</b></p>			
<b>1. REPORT DATE (DD-MM-YYYY)</b> 10-04-2020		<b>2. REPORT TYPE</b> Final Performance	
<b>3. DATES COVERED (From - To)</b> 01 Sep 2016 to 31 Aug 2019			
<b>4. TITLE AND SUBTITLE</b> LES Modeling of Non-local effects using Statistical Coarse-graining		<b>5a. CONTRACT NUMBER</b>	
		<b>5b. GRANT NUMBER</b> FA9550-16-1-0309	
		<b>5c. PROGRAM ELEMENT NUMBER</b> 61102F	
<b>6. AUTHOR(S)</b> Karthik Duraisamy		<b>5d. PROJECT NUMBER</b>	
		<b>5e. TASK NUMBER</b>	
		<b>5f. WORK UNIT NUMBER</b>	
<b>7. PERFORMING ORGANIZATION NAME(S) AND ADDRESS(ES)</b> REGENTS OF THE UNIVERSITY OF MICHIGAN 503 THOMPSON ST ANN ARBOR, MI 48109-1340 US		<b>8. PERFORMING ORGANIZATION REPORT NUMBER</b>	
<b>9. SPONSORING/MONITORING AGENCY NAME(S) AND ADDRESS(ES)</b> AF Office of Scientific Research 875 N. Randolph St. Room 3112 Arlington, VA 22203		<b>10. SPONSOR/MONITOR'S ACRONYM(S)</b> AFRL/AFOSR RTA2	
		<b>11. SPONSOR/MONITOR'S REPORT NUMBER(S)</b> AFRL-AFOSR-VA-TR-2020-0045	
<b>12. DISTRIBUTION/AVAILABILITY STATEMENT</b> A DISTRIBUTION UNLIMITED: PB Public Release			
<b>13. SUPPLEMENTARY NOTES</b>			
<b>14. ABSTRACT</b> The development of coarse-grained and reduced-complexity simulation models continues to be a pacing research challenge in computational physics. For instance, state-of-the-art techniques such as Large Eddy Simulation models are still not effective in many flows -- such as turbulent combustion -- in which sub-filter scales have a significant impact on transport processes. The major obstacle is to effectively reconcile the loss of information in the coarse-graining process and numerical discretization. The broad goal of our work is to approach multiscale/multi-physics modeling with: 1. Minimal heuristics and phenomenology 2. Consideration of numerical implementation 3. Algorithmic efficiency 4. Provable (non-linear) stability 5. Scalable implementation 6. Applicability to complex discretizations 7. Applicable to arbitrarily complex physics/PDEs We pursue several lines of attack towards this end, leveraging...			
<b>15. SUBJECT TERMS</b> LES, Mori-Zwanzig, multiscale			
<b>16. SECURITY CLASSIFICATION OF:</b>			

Standard Form 298 (Rev. 8/98)  
Prescribed by ANSI Std. Z39.18

DISTRIBUTION A: Distribution approved for public release

<b>a. REPORT</b> Unclassified	<b>b. ABSTRACT</b> Unclassified	<b>c. THIS PAGE</b> Unclassified	<b>17. LIMITATION OF ABSTRACT</b>  UU	<b>18. NUMBER OF PAGES</b>	<b>19a. NAME OF RESPONSIBLE PERSON</b> FAHROO, FARIBA
					<b>19b. TELEPHONE NUMBER</b> <i>(Include area code)</i> 703-696-8429

# LES Modeling of Non-local Effects using Statistical Coarse-graining

Principal Investigator: Karthik Duraisamy

Co-Principal Investigator: Venkat Raman

## Executive summary

The development of coarse-grained and reduced-complexity simulation models continues to be a pacing research challenge in computational physics. For instance, state-of-the-art techniques such as Large Eddy Simulation models are still not effective in many flows – such as turbulent combustion – in which sub-filter scales have a significant impact on transport processes. The major obstacle is to effectively reconcile the loss of information in the coarse-graining process and numerical discretization. The broad goal of our work is to approach multiscale/multi-physics modeling with:

- Minimal heuristics and phenomenology
- Consideration of numerical implementation
- Algorithmic efficiency
- Provable (non-linear) stability
- Scalable implementation
- Applicability to complex discretizations
- Applicable to arbitrarily complex physics/PDEs

We pursue several lines of attack towards this end, leveraging and further developing recent advances in mathematical formalisms to obtain physically and numerically consistent models. Demonstrations are performed on a spectrum of problems ranging from simple dynamical systems to turbulence to multi-physics simulations. The main focus of this project is the establishment of a paradigm for multiscale modeling that combines the Mori-Zwanzig (MZ) formalism of Statistical Mechanics with the Variational Multiscale (VMS) method. The MZ-VMS approach leverages both VMS scale-separation projectors as well as phase-space projectors to provide a systematic modeling approach that is applicable to non-linear partial differential equations. The MZ-VMS framework leads to a closure term that is non-local in time and appears as a convolution or memory integral. The resulting non-Markovian system is used as a starting point for model development. A major contribution of this work is that we have been able to unravel some of the complexities of MZ-based modeling and make it accessible to the broader computational science community.

**Significant accomplishments:**

- Developed a parameter-free predictive MZ closure, the dynamic-MZ- $\tau$  model. This technique has similarities to the dynamic Smagorinsky model of turbulence, but the functional form comes from math and not physics.
- Discovery that for the finite memory model, the memory term is driven by both an orthogonal projection of the coarse-scale residual and jumps at element interfaces. This insight provides the first links between MZ-based models and existing stabilization techniques.
- MZ formulation for Spectral, Finite Element (Continuous & Discontinuous Galerkin), & Projection-based reduced order models for PDEs
- For discontinuous Galerkin method (for compressible NS), an establishment of connections between MZ-based methods, upwinding, and artificial viscosity.
- Developed efficient a priori strategy to extract memory kernels from an ensemble of targeted fine scale simulations.
- First development/application of MZ-based techniques to wall bounded turbulent flows, to Discontinuous Galerkin, Magnetohydrodynamic turbulence, and combustion.
- the MZ-VMS technique is intimately connected to the numerical discretization. The search for the ideal fully resolved model (i.e. before coarse-graining) for compressible flows led us to entropy conservative methods. Consequently, we developed entropy-stable and entropy conservative formulations for multi-component flows. We also proved an minimum entropy principle for the multicomponent compressible Euler equations.
- As an off-shoot of the above work, our search for the ideal MZ closure led us to non-local (temporal memory) data-driven closures and reduced order modeling using approximate inertial manifolds and convolutional neural networks.

## Publications

1. Parish, E., Duraisamy, K., A Dynamic Sub-grid Scale Model for Large Eddy Simulations based on the Mori-Zwanzig formalism,” *Journal of Computational Physics*, Vol. 349, 2017.
2. Gouasmi, A., Parish, E., Duraisamy, K., A Priori Estimation of Memory Effects in Reduced Order Modeling of Nonlinear Systems Using the Mori-Zwanzig formalism, *Proc. Royal Soc. Ser A*, Vol. 473, 2017.
3. Pan. S., Duraisamy, K., “Data-driven Discovery of Closure Models,” *SIAM Journal on Applied Dynamical Systems*, 2018.
4. Pan. S., and Duraisamy, K., “Long-time predictive modeling of nonlinear dynamical systems using neural networks,” *Complexity*, 2018.
5. Gouasmi, A., Murman, S., Duraisamy, K., Entropy Conservative Schemes and the Receding Flow Problem, *Journal of Scientific Computing*, 2019.
6. Hassanaly, A., and Raman, V., Emerging trends in numerical simulations of combustion systems, M. Hassanaly and V. Raman, *Proceedings of the Combustion Institute*, 2019.

7. Barwey, S., Hassanaly, M., An, Q., Raman, V., Steinberg, A., Experimental data-based reduced-order model for analysis and prediction of flame transition in gas turbine combustors, *Combustion theory and modeling*, 2019.
8. Gouasmi, A., Duraisamy, K., Murman, S., Tadmor, E., A minimum entropy principle in the compressible multicomponent Euler equations, *ESAIM: Mathematical Modelling and Numerical Analysis*, 2019.
9. Parish, E., and Duraisamy, K., A Unified Framework for Multiscale Modeling using the Mori-Zwanzig Formalism and the Variational Multiscale Method,” arXiv:1712.09669, 2018.
10. Gouasmi, A., Murman, S., Duraisamy, K., On Entropy stable temporal fluxes, arXiv:1807.03483, 2018.
11. Pradhan, A., Duraisamy, K., Variational Multiscale Closures for Finite Element Discretizations Using the Mori-Zwanzig Approach, arXiv:1906.01411, 2019.
12. Gouasmi, A., Duraisamy, K., Murman, S., Formulation of Entropy-Stable schemes for the multicomponent compressible Euler equations, arXiv:1904.00972, 2019.
13. Parish, E., Wentland, C., Duraisamy, K., The Adjoint Petrov-Galerkin Method for Non-Linear Model Reduction, arXiv:1810.03455, 2019.
14. M. Akram, M. Hassanaly, V. Raman, A priori analysis of reduced description of dynamical systems by approximate inertial manifolds (AIM), 2019.

#### **PhD Theses**

1. Parish, E., Variational Multiscale Modeling and Memory Effects in Turbulent Flow Simulations, Dept of Aerospace Engineering, Univ of Michigan, Ann Arbor, 2018. *Subsequently, John Von Neumann Fellow at Sandia National Labs.*
2. Gouasmi, A., Contributions to the Development of Entropy-Stable Schemes for Compressible Flows, Dept of Aerospace Engineering, Univ of Michigan, Ann Arbor, 2019. *Subsequently, NASA Post Doctoral Fellow.*

# 1 Introduction

Future aircraft engines as well as secondary combustion systems (for instance, augmentors) will increasingly rely on highly turbulent burning of molecularly premixed fuel/air mixtures. Such systems can bring down emissions levels dramatically, but are subject to combustion instabilities, a situation in which there exist strong interactions between flame propagation, heat release, turbulent flow and acoustics. Numerical simulation techniques have the potential to augment our theoretical understanding in the above problems and ultimately serve as a design tool. The central challenge in simulations of the aforementioned turbulence and combustion phenomena arises from the need to represent an enormous disparity of time and length scales which makes direct numerical simulations impractical in realistic problems. There is thus a need for models that can efficiently represent transport, chemical kinetics and the interaction of turbulence and chemistry. It is well-accepted that approaches based on Large Eddy Simulations (LES) represent the minimum required fidelity to capture the relevant physics.

LES is a powerful approach for simulating complex turbulent and reacting flows of interest to propulsion applications. The traditional approach to LES is to apply a low-pass filter to the governing equations, generating resolved and unresolved terms. Transport equations are solved for the resolved terms, while the unresolved terms are modeled using the resolved field. Traditional closure methodologies for LES utilize simple models evoking effective subgrid “viscosity” type arguments (or rely on numerical dissipation) to represent the unresolved stresses that result from the filtering process. *These subgrid-scale (SGS) models have been successful in problems in which the resolved scales drive the dominant transport processes.* In many other problems – such as in the near-wall region of a turbulent boundary layer – the necessary resolution required of a high-quality LES renders such simulations prohibitively expensive unless a high degree of empiricism is introduced into the modeling process. Further, since combustion occurs exclusively at the small scales, the influence of chemical reactions and unresolved turbulence on the large-scale flow evolution requires careful consideration.

In general, theoretical developments and semi-empirical models have thus far provided insights and qualitative connections to parameters and phenomena from unresolved scales. It is well-argued that for LES to be sufficiently accurate at a reasonable cost, there needs to be a closer link between the SGS model and the mathematics of the filtering/coarse-graining process. Such a predictive capability that also consistently couples information across multiple scales from sub-grid to poorly-resolved to well-resolved is of critical importance and is the target of the proposed work.

This project advances our fundamental understanding of multiscale modeling and develops a rigorous modeling framework by combining the Mori-Zwanzig (MZ) formalism of statistical mechanics with the variational multiscale (VMS) method. This approach leverages scale-separation projectors as well as phase-space projectors to provide a systematic modeling approach that is applicable to complex non-linear partial differential equations. A schematic of the approach is shown in Figure 1. The rest of this document provides background, discussion and some highlights of the developments in this project.

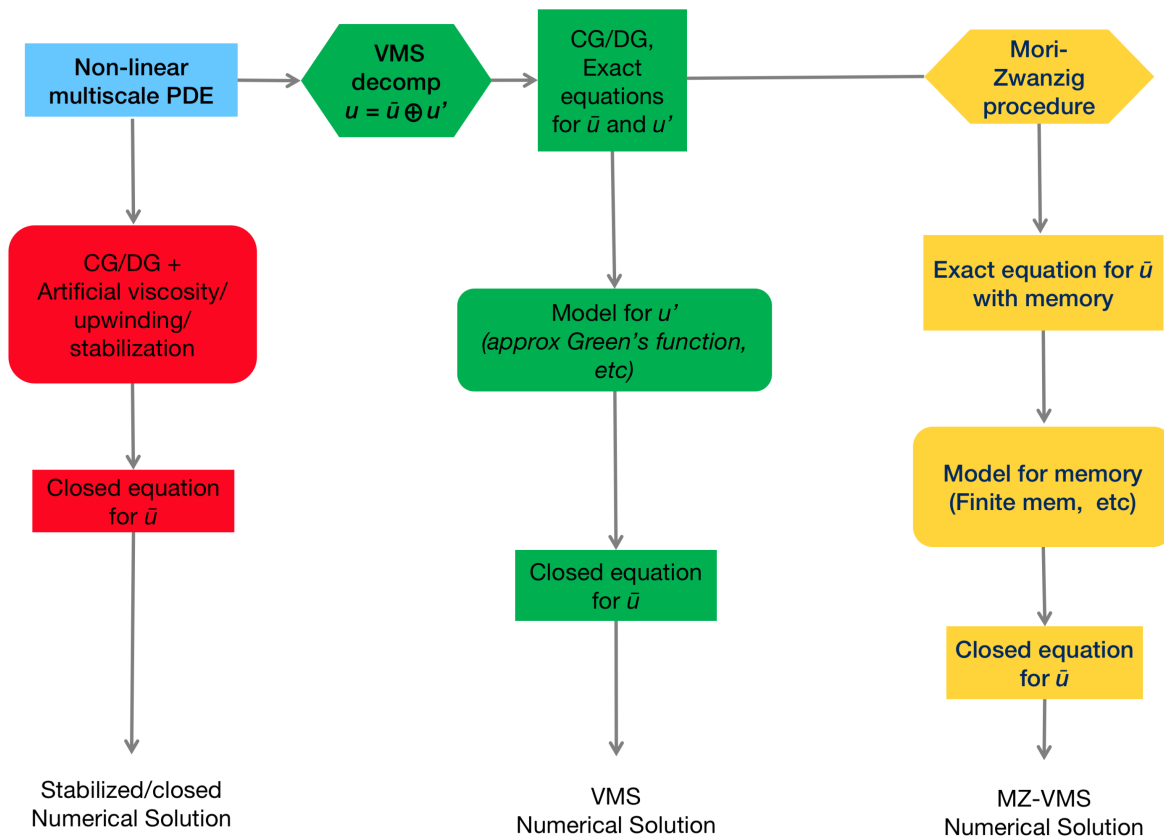


Figure 1: Schematic of the use of the Mori-Zwanzig formalism as a procedure for multiscale modeling. *Rectangles*: Equations, *6-sided figures*: Mathematical procedure, *Rounded rectangles*: Modeling assumptions.



## 2 Multiscale Decomposition

We consider the initial-value problem

$$\frac{\partial u}{\partial t} = \mathcal{R}(u) \quad x \in \Omega, t \in (0, T), \quad (1)$$

where the operator  $\mathcal{R}$  is a linear or non-linear differential operator. The governing equations are subject to boundary and initial conditions,

$$u(x, t) = 0 \quad x \in \Gamma, t \in (0, T), \quad (2)$$

$$u(x, 0) = u_0 \quad x \in \Omega. \quad (3)$$

We focus on weighted residual solutions to Eq. 1, which requires defining a test and trial space. Let  $\mathcal{V} \equiv H_0^1(\Omega)$  denote the trial space and  $\mathcal{W}$  the test space. The weighted residual problem is defined as follows: find  $u \in \mathcal{V}$  such that  $\forall w \in \mathcal{W}$ ,

$$\left( w, \frac{\partial u}{\partial t} \right) = \left( w, \mathcal{R}(u) \right). \quad (4)$$

### 2.1 Variational Multiscale Method

The variational multiscale method utilizes a decomposition of the solution space into a coarse-scale resolved space  $\tilde{\mathcal{V}} \subset \mathcal{V}$  and a fine-scale unresolved space  $\mathcal{V}' \subset \mathcal{V}$ . In VMS, the solution space is expressed as a sum decomposition,

$$\mathcal{V} = \tilde{\mathcal{V}} \oplus \mathcal{V}'. \quad (5)$$

Let  $\tilde{\Pi}$  be the linear projector onto the coarse-scale space,  $\tilde{\Pi} : \mathcal{V} \rightarrow \tilde{\mathcal{V}}$ . Various choices exist for the projector  $\tilde{\Pi}$ , and here we exclusively consider  $\tilde{\Pi}$  to be the  $L^2$  projector,

$$(\tilde{w}, \tilde{\Pi}u) = (\tilde{w}, u), \quad \forall \tilde{w} \in \tilde{\mathcal{V}}, u \in \mathcal{V}.$$

The fine-scale space,  $\mathcal{V}'$ , becomes the orthogonal complement of  $\tilde{\mathcal{V}}$  in  $\mathcal{V}$  such that,

$$(\tilde{w}, \Pi'u) = 0 \quad \forall \tilde{w} \in \tilde{\mathcal{V}}, u \in \mathcal{V},$$

where  $\Pi' = \mathbf{I} - \tilde{\Pi}$ . With this decomposition, the solution can be represented as,

$$u = (\tilde{\Pi} + \Pi')u = \tilde{u} + u',$$

and the same for  $w$ . It is assumed that  $\tilde{u}$  and  $u'$  are homogeneous on  $\Gamma$ . By virtue of the linear independence of the fine and coarse trial spaces, governing equations can be separated into two sub-problems,

$$(\tilde{w}, \tilde{u}_t) = (\tilde{w}, \mathcal{R}(\tilde{u} + u')), \quad \forall \tilde{w} \in \tilde{\mathcal{V}} \quad (6)$$

$$(w', u'_t) = (w', \mathcal{R}(\tilde{u} + u')), \quad \forall w' \in \mathcal{V}' \quad (7)$$

$$\tilde{u}(x, t) = 0, \quad u'(x, t) = 0, \quad x \in \Gamma, t \in (0, T), \quad (8)$$

$$\tilde{u}(x, 0) = \tilde{u}_0, \quad u'(x, 0) = 0, \quad x \in \Omega. \quad (9)$$

The philosophy of VMS is to develop an approximation for the fine-scale state,  $u'$ , and inject it into the coarse-scale equation.

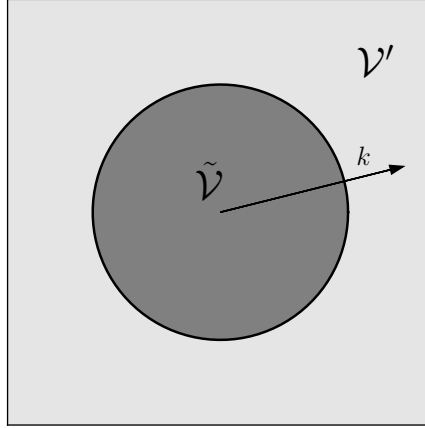


Figure 2: Graphical illustration of the decomposition of the solution space  $\mathcal{V}$  into subspaces  $\tilde{\mathcal{V}}$  and  $\mathcal{V}'$  in the frequency domain. The wavenumber is  $k$ . The subspace  $\tilde{\mathcal{V}}$  corresponds to the low frequency, "coarse-scale" subspace and is resolved in a numerical method. The subspace  $\mathcal{V}'$  is the high frequency "fine-scale" subspace and is not resolved in a numerical method. We consider a decomposition that obeys  $\mathcal{V} = \tilde{\mathcal{V}} \oplus \mathcal{V}'$ , with  $\mathcal{V}'$  being  $L^2$  orthogonal to  $\tilde{\mathcal{V}}$ .

### 3 Mori-Zwanzig Formalism

#### 3.1 Semi-Discrete Setting

#### 3.2 Transformation to Phase Space and the Liouville Equation

The integrating factor approach described in the previous section relies on the principle of superposition and is limited to linear systems. The MZ procedure addresses non-linearity by casting the original semi-discrete Galerkin system as a partial differential equation that exists in phase space. It is worth emphasizing that, although the Mori-Zwanzig formalism has its roots in the work of Mori and Zwanzig, the work of Chorin and collaborators<sup>5,7,10</sup> is a significant revamp of the formalism and extends the concept to general systems of ordinary differential equations. The following discussion is inspired by<sup>5</sup> and we refer the reader to both<sup>5</sup> and<sup>6</sup> for clarification on any of the following points.

To formally remove the fine-scale variables, the Mori-Zwanzig approach is used. The starting point for the approach is to transform the ODE system into a linear partial differential equation,

$$\frac{\partial}{\partial t} v(\mathbf{a}_0, t) = \mathcal{L}v(\mathbf{a}_0, t); \quad v(\mathbf{a}_0, 0) = g(\mathbf{a}_0), \quad (10)$$

where  $\mathcal{L}$  is the Liouville operator and is given by,

$$\mathcal{L} = \sum_{j=0}^{\infty} (w_j, \mathcal{R}(u_0)) \frac{\partial}{\partial a_{0j}}. \quad (11)$$

Equation 10 is referred to as the Liouville equation and is an exact statement of the original dynamics. The Liouville equation describes the solution to Eq. 1 for *all* possible initial condi-

tions. The advantage of reformulating the system in this way is that the Liouville equation is linear. This linearity allows for the use of superposition and aids in the formal removal of the fine scales.

The solution to Eq. 10 can be written as,

$$v(\mathbf{a}_0, t) = e^{t\mathcal{L}}g(\mathbf{a}(\mathbf{a}_0, 0)). \quad (12)$$

The operator  $e^{t\mathcal{L}}$ , which has been referred to as a ‘‘propagator’’, evolves the solution along its trajectory in phase-space. The operator  $e^{t\mathcal{L}}$  has several interesting properties. Most notably, the operator can be ‘‘pulled’’ inside of a non-linear functional,

$$e^{t\mathcal{L}}g(\mathbf{a}(\mathbf{a}_0, 0)) = g(e^{t\mathcal{L}}\mathbf{a}(\mathbf{a}_0, 0)). \quad (13)$$

This is similar to the composition property inherent to Koopman operators<sup>19</sup>. With this property, the solution to Eq. 10 may be written as,

$$v(\mathbf{a}_0, t) = g(e^{t\mathcal{L}}\mathbf{a}(\mathbf{a}_0, 0)). \quad (14)$$

The implications of  $e^{t\mathcal{L}}$  are significant. It demonstrates that, given the trajectories  $\mathbf{a}(\mathbf{a}_0, t)$ , the solution  $v$  is known for any observable  $g$ . Noting that  $\mathcal{L}$  and  $e^{t\mathcal{L}}$  commute, Eq. 10 may be written in the semi-group notation as,

$$\frac{\partial v}{\partial t} = e^{t\mathcal{L}}\mathcal{L}v(\mathbf{a}_0, 0). \quad (15)$$

A set of equations for the resolved modes can be obtained by taking  $g(\mathbf{a}_0, 0) = \tilde{\mathbf{a}}_0$ ,

$$\frac{\partial}{\partial t}e^{t\mathcal{L}}\tilde{\mathbf{a}} = e^{t\mathcal{L}}\mathcal{L}\tilde{\mathbf{a}}. \quad (16)$$

### 3.2.1 Projection Operators and the Liouville Equation

We proceed by decomposing the Hilbert space  $\mathcal{H}$ , into a resolved and unresolved subspace,

$$\mathcal{H} = \tilde{\mathcal{H}} \oplus \mathcal{H}'. \quad (17)$$

The associated projection operators are defined as  $\mathcal{P} : \mathcal{H} \rightarrow \tilde{\mathcal{H}}$  and  $\mathcal{Q} = I - \mathcal{P}$ . The following projection operator is considered,

$$\mathcal{P}f(\tilde{\mathbf{a}}_0, \mathbf{a}'_0) = \int_{\mathcal{H}} f(\tilde{\mathbf{a}}_0, \mathbf{a}'_0)\delta(\mathbf{a}'_0)d\mathbf{a}'_0, \quad (18)$$

which leads to

$$\mathcal{P}f(\tilde{\mathbf{a}}_0, \mathbf{a}'_0) = f(\tilde{\mathbf{a}}_0, 0). \quad (19)$$

The projectors  $\mathcal{P}$  and  $\mathcal{Q}$  are orthogonal to each other. Other projections, such as conditional expectations are possible<sup>5</sup>, but will not be pursued in the present work. It is important to emphasize that the projectors  $\mathcal{P}$  and  $\mathcal{Q}$  operate on functions of  $\mathcal{H}$  and are fundamentally different from the  $L^2$  projectors  $\tilde{\Pi}$  and  $\Pi'$ . With the projection operators, the Liouville equation can be split as,

$$\frac{\partial}{\partial t}e^{t\mathcal{L}}\tilde{\mathbf{a}}_0 = e^{t\mathcal{L}}\mathcal{P}\mathcal{L}\tilde{\mathbf{a}}_0 + e^{t\mathcal{L}}\mathcal{Q}\mathcal{L}\tilde{\mathbf{a}}_0. \quad (20)$$

The objective now is to remove the dependence of the right hand side of Eq. 20 on the unresolved scales,  $\mathbf{a}'$  (i.e.  $\mathcal{Q}\mathcal{L}\tilde{\mathbf{a}}$ ). To demonstrate how this may be achieved, consider the partial differential operator governed by the semigroup  $e^{t\mathcal{L}}$  written as,

$$\frac{\partial}{\partial t} - \mathcal{L} = 0. \quad (21)$$

We will refer to Eq. 21 as the homogeneous problem. Consider now the inhomogeneous problem with forcing  $\mathcal{P}\mathcal{L}$ ,

$$\frac{\partial}{\partial t} - \mathcal{L} = -\mathcal{P}\mathcal{L}. \quad (22)$$

Making use of the identity  $I = \mathcal{P} + \mathcal{Q}$ , the inhomogeneous problem can be written as

$$\frac{\partial}{\partial t} - \mathcal{Q}\mathcal{L} = 0. \quad (23)$$

Eq. 23 is referred to in the literature as the orthogonal dynamics operator, and can be conceptualized as a Liouville operator with forcing. The evolution operator given by the orthogonal dynamics is  $e^{t\mathcal{Q}\mathcal{L}}$ . Here, we can leverage the linearity of the partial differential operators and make use of superposition. The solution to the orthogonal dynamics equation can be expressed in terms of solutions to the homogeneous Liouville equation through Duhamel's principle (in operator form),

$$e^{t\mathcal{L}} = e^{t\mathcal{Q}\mathcal{L}} + \int_0^t e^{(t-s)\mathcal{L}}\mathcal{P}\mathcal{L}e^{s\mathcal{Q}\mathcal{L}}ds. \quad (24)$$

Inserting Eq. 24 into Eq. 20, the generalized Langevin equation is obtained,

$$\frac{\partial}{\partial t}e^{t\mathcal{L}}\tilde{\mathbf{a}}_0 = \underbrace{e^{t\mathcal{L}}\mathcal{P}\mathcal{L}\tilde{\mathbf{a}}_0}_{\text{Markovian}} + \underbrace{e^{t\mathcal{Q}\mathcal{L}}\mathcal{Q}\mathcal{L}\tilde{\mathbf{a}}_0}_{\text{Noise}} + \underbrace{\int_0^t e^{(t-s)\mathcal{L}}\mathcal{P}\mathcal{L}e^{s\mathcal{Q}\mathcal{L}}\mathcal{Q}\mathcal{L}\tilde{\mathbf{a}}_0ds}_{\text{Memory}}. \quad (25)$$

The system described in Eq. 25 is precise and not an approximation to the original ODE system. For notational purposes, define

$$F_j(\mathbf{a}_0, t) = e^{t\mathcal{Q}\mathcal{L}}\mathcal{Q}\mathcal{L}\mathbf{a}_0, \quad K_j(\mathbf{a}_0, t) = \mathcal{P}\mathcal{L}F_j(\mathbf{a}_0, t). \quad (26)$$

We refer to  $K(\mathbf{a}_0, t)$  as the memory kernel. It can be shown that solutions to the orthogonal dynamics equation are in the null space of  $\mathcal{P}$ , meaning  $\mathcal{P}F_j(\mathbf{a}_0, t) = 0$ . By the definition of fully resolved initial conditions, the noise-term is zero and we obtain,

$$\frac{\partial}{\partial t}e^{t\mathcal{L}}\tilde{\mathbf{a}}_0 = e^{t\mathcal{L}}\mathcal{P}\mathcal{L}\tilde{\mathbf{a}}_0 + \int_0^t e^{(t-s)\mathcal{L}}\mathcal{P}\mathcal{L}e^{s\mathcal{Q}\mathcal{L}}\mathcal{Q}\mathcal{L}\tilde{\mathbf{a}}_0ds. \quad (27)$$

Equation 27 can be written in a more transparent form,

$$(\tilde{\mathbf{w}}, \tilde{u}_t) = (\tilde{\mathbf{w}}, \mathcal{R}(\tilde{u})) + \int_0^t K(\tilde{\mathbf{a}}(t-s), s)ds, \quad (28)$$

where  $K_j(\mathbf{a}_0, t) = \mathcal{P}\mathcal{L}e^{t\mathcal{Q}\mathcal{L}}\mathcal{Q}\mathcal{L}\mathbf{a}_0$ . Note that the time derivative is represented as a partial derivative due to the Liouville operators embedded in the memory.

*Remarks*

1. Equation 28 is precisely a Galerkin discretization of Eq. 1 with the addition of a memory term originating from scale separation.
2. Equation 28 is a non-local closed equation for the coarse-scales.
3. Evaluation of the memory term is not tractable as it involves the solution of the evolution operator,  $e^{t\mathcal{Q}\mathcal{L}}$ . This is referred to as the orthogonal dynamics and is discussed in the following section. Instead, Eq. 28 is viewed as a starting point for the construction of closure models.

## 4 The Memory Term: Insight and Modeling

The MZ-VMS procedure itself does not provide a reduction in computational complexity as it has replaced the fine-scale state with a memory term. This memory term relies on solutions to the orthogonal dynamics equation, which is intractable in the general case. The MZ-VMS procedure instead provides an exact representation of the fine-scale state in terms of the coarse-scales. This is used as a starting point for model development. In this section, we expand our discussion of the orthogonal dynamics equation and discuss several modeling strategies. In particular we discuss the value of the memory kernel at  $s = 0$  and demonstrate that many existing MZ models are residual-based closures.

### 4.1 The orthogonal dynamics

In the Variational Multiscale method, the fine-scale state is parameterized in terms of the coarse-scale state by virtue of a fine-scale Green's function. The Mori-Zwanzig procedure instead uses Duhamel's principle to relate the solution of the orthogonal dynamics equation to the Liouville equation. This allows for the elimination of fine-scales. The evolution operator of the orthogonal dynamics is given by  $e^{t\mathcal{Q}\mathcal{L}}$ . It is important to recognize that, while the evolution operator  $e^{t\mathcal{L}}$  is a Koopman operator, no such result exists for  $e^{t\mathcal{Q}\mathcal{L}}$  in the general non-linear case. As a consequence, evaluating terms evolved by  $e^{t\mathcal{Q}\mathcal{L}}$  requires one to directly solve the orthogonal dynamics equation. This is, in general, intractable.

To help clarify the interaction of the memory term and the orthogonal dynamics, Figure 3 depicts the memory term in  $s - t$  space. In Figure 3a, the evolution of the solution in time is denoted by the solid blue line at  $s = 0$ . To evaluate the memory, solutions to the orthogonal dynamics equation,  $F(\tilde{\mathbf{a}}(t), s)$ , must be evolved in pseudo-time  $s$  using initial conditions that depend on the solution at time  $t$ . This is depicted by the dashed red lines in Figure 3. This leads to a three-dimensional surface in  $s - t$  space, as seen in Figure 3. Evaluation of the memory integral then requires a path integration backwards in time along the dashed-lines in Figure 3a, yielding the shaded yellow region in Figure 3b.

A quantity that is of particular interest is the memory kernel evaluated at  $s = 0$ , which is denoted by the solid blue line. This term,  $K(\tilde{\mathbf{a}}(t), 0)$ , drives the memory term and is typically leveraged to develop closure models<sup>17,20</sup> within the MZ setting. A clear derivation for the smooth case is presented in Ref. 21 and we present the important result,

$$K(\tilde{\mathbf{a}}(t), 0) = \int_{\Omega} \int_{\Omega} (\tilde{\mathbf{w}}\mathcal{R}') (x) \Pi'(x, y) (\mathcal{R}(\tilde{u}) - f)(y) d\Omega_y d\Omega_x, \quad (29)$$

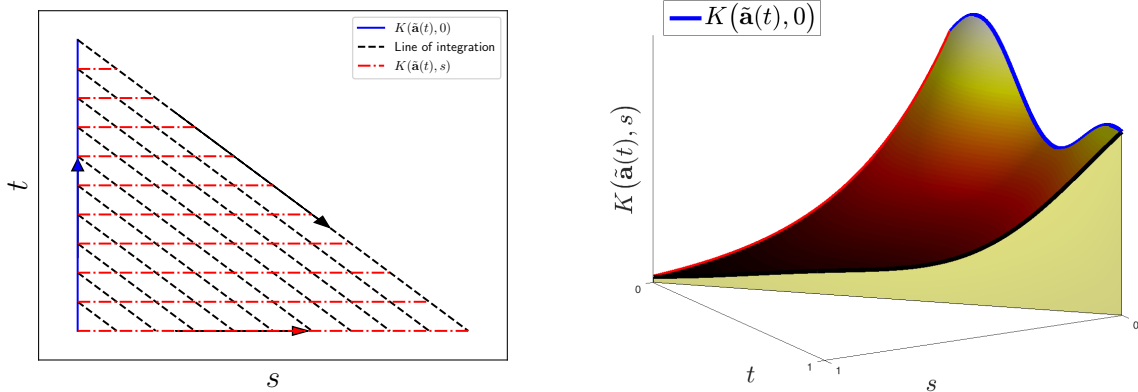


Figure 3: Graphical depiction of the mechanics of the memory term.

where  $\mathcal{R}' = \frac{\partial \mathcal{R}}{\partial \tilde{u}}$ .

*Remarks*

1. Equation 29 shows that the memory is driven by an orthogonal projection of the coarse-scale residual. If this residual is zero, no information is added to the memory. Further, if the coarse-scale residual is fully resolved, no information is added to the memory.

## 4.2 Models for the Memory

The construction of an appropriate surrogate to the memory term requires an understanding of the structure of the orthogonal dynamics equation. Due to the challenges associated with the solution of very high-dimensional partial differential equations, to the knowledge of the authors no direct attempt has been undertaken to solve the orthogonal dynamics equation. The most general attempt to extract the memory term and orthogonal dynamics is presented in<sup>5</sup>, where Hermite polynomials and Volterra integral equations are used to approximate the memory (and hence orthogonal dynamics). This procedure was shown to provide a reasonably accurate representation of the memory for a low-dimensional dynamical system. The procedure, however, is intractable for high-dimensional problems. This fact is exemplified in the work of Bernstein<sup>3</sup>, where the methodology is applied to the Burgers equation.

In Gouasmi et al.<sup>15</sup> we extract the memory by assuming that the semi-group emerging from the orthogonal dynamics equation is a composition operator. This allows the orthogonal dynamics to be solved by virtue of an auxiliary set of ordinary differential equations. This method was shown to be exact for linear systems. It further provided reasonable results for mildly non-linear problems and suggested the presence of finite memory effects. The success of the method, however, is problem-dependent and its accuracy is challenging to assess, from a theoretical standpoint.

Despite the complexity and minimal understanding of the orthogonal dynamics, various surrogate models for the memory exist. These models are typically based on series expansions or geometrical arguments and have been applied to problems of varying complexity. The majority

of analytic models for the MZ memory term involve repeated applications of projection and Liouville operators. These may be written as,

$$e^{t\mathcal{L}}\mathcal{P}\mathcal{L}(\mathcal{Q}\mathcal{L})^n\tilde{\mathbf{a}}_0 = \left( \tilde{\mathbf{w}}, (\mathcal{R}'\Pi')^n\mathcal{R}(\tilde{u}) \right)$$

$$e^{t\mathcal{L}}(\mathcal{P}\mathcal{L})^n\mathcal{Q}\mathcal{L}\tilde{\mathbf{a}}_0 = \left( \tilde{\mathbf{w}}, \mathcal{R}'\Pi'(\mathcal{R}'\tilde{\Pi})^{n-1}\mathcal{R}(\tilde{u}) \right).$$

#### 4.2.1 The $\tau$ -model

The  $\tau$ -model is structurally equivalent to Chorin's original  $t$ -model, but contains a different time-scale that is motivated by the idea that memory has a finite support in time. The model is given by,

$$\int_0^t K(\tilde{\mathbf{a}}(t-s), s) ds \approx \tau \left( \tilde{\mathbf{w}}, \mathcal{R}'\Pi'\mathcal{R}(\tilde{u}) \right). \quad (30)$$

where  $\tau$  is the memory length. We developed a dynamic procedure to compute  $\tau$  in Ref. 20. The methodology leverages the Germano identity and assumes scale similarity to construct an energy transfer constraint between two-levels of coarse-graining. The appeal of the proposed model, which we refer to as the dynamic-MZ- $\tau$  model, is that it is parameter-free and has a structural form imposed by the mathematics of the coarse-graining process (rather than the phenomenological assumptions made by the modeler, such as in classical subgrid scale models). To promote the applicability of M-Z models in general, we present two procedures to compute the resulting model form, helping to bypass the tedious error-prone algebra that has proven to be a hindrance to the construction of M-Z-based models for complex dynamical systems. We have demonstrated the model in the context of Large Eddy Simulation closures for Burgers equation, rotating turbulence, Magneto-hydro dynamic turbulence, and turbulent channel flow.

## 5 Connections of MZ-VMS with Existing Concepts

In Section 4, it was seen that all models utilize the term  $K(\tilde{\mathbf{a}}(t), 0)$ , which is written equivalently as  $e^{t\mathcal{L}}\mathcal{P}\mathcal{L}\mathcal{Q}\mathcal{L}\tilde{\mathbf{a}}_0$ . This value drives the memory term and has been discussed throughout the previous sections. We consider the memory kernel at  $s = 0$  for the FEM case. Recall that this term appears as

$$\begin{aligned} \tilde{\mathbf{M}}K(\tilde{\mathbf{a}}(t), 0) &= \int_{\Omega} \int_{\Omega} (\tilde{\mathbf{w}}\mathcal{R}')(x)\Pi'(x, y)(\mathcal{R}(\tilde{u}) - f)(y)d\Omega_y d\Omega_x \\ &+ \int_{\Omega} \int_{\Gamma} (\tilde{\mathbf{w}}\mathcal{R}')(x)\Pi'(x, y)b(\tilde{u}(y))d\Gamma_y d\Omega_x \\ &+ \int_{\Gamma} \int_{\Omega} (\tilde{\mathbf{w}}b')(x)\Pi'(x, y)(\mathcal{R}(\tilde{u}) - f)(y)d\Gamma_y d\Omega_x \\ &+ \int_{\Gamma} \int_{\Gamma} (\tilde{\mathbf{w}}b')(x)\Pi'(x, y)b(\tilde{u}(y))d\Gamma_y d\Gamma_x, \end{aligned} \quad (31)$$

where  $\mathcal{R}' = \frac{\partial \mathcal{R}}{\partial \tilde{u}}$  and  $b' = \frac{\partial b}{\partial \tilde{u}}$ . The term  $\Pi'$  is the  $L^2$  projection onto the fine-scales,

$$\Pi'(x, y) = \mathbf{w}'^T(x)\mathbf{M}'^{-1}\mathbf{w}'(y). \quad (32)$$

*Remarks*

1. The memory is driven by the residual of the coarse-scales projected onto  $\mathcal{V}'$ . When the residual of the coarse-scales is negligible, no additional information is added to the memory. Models such as the  $t$  and  $\tau$ -model are inactive. Further, if the coarse-scale residual is non-zero but exists only in  $\tilde{\mathcal{V}}$ , models such as the  $t$  and  $\tau$ -model are again inactive and no information is added to the memory.
2. The orthogonal projection,  $\Pi'$ , can be conceptualized as a mechanism to enforce the approximation to constrain the fine-scale state to the correct trial space,  $\mathcal{V}'$ . A significant body of work on orthogonal subgrid-scale models in the context of the Variational Multi-scale Method has been undertaken by Codina<sup>8,9,16,2</sup>.
3. The boundary terms in the FEM formulation give rise to surface integrals. As will be shown later, these surface integrals can, in turn, give rise to jump operators between elements and can add artificial diffusion to the system.
4. It is seen that the orthogonal projector,  $\Pi'(x, y)$ , can be viewed as an approximation to the fine-scale Green's function. This will be discussed in the next section.

### 5.1 The $\tau$ -model and an orthogonal approximation to the fine-scale Green's function

Approximating the memory with the  $\tau$ -model gives rise to the following closed equations for the coarse-scales,

$$(\tilde{\mathbf{w}}, \tilde{u}_t) + (\tilde{\mathbf{w}}, \mathcal{R}(\tilde{u})) - \tau \tilde{\mathbf{M}}K(\tilde{\mathbf{a}}(t), 0) = (\tilde{\mathbf{w}}, f). \quad (33)$$

### 5.2 Residual-Based Artificial Viscosity

To further clarify the role of the  $e^{t\mathcal{L}}\mathcal{P}\mathcal{L}\mathcal{Q}\mathcal{L}\tilde{\mathbf{a}}_0$  term, we consider the hyperbolic conservation law,

$$\frac{\partial \mathbf{u}}{\partial t} + \nabla \cdot \mathbf{F}(\mathbf{u}) = 0 \quad \text{in} \quad \Omega. \quad (34)$$

The semi-discrete system obtained through the FEM discretization is,

$$\int_{\Omega} \mathbf{w} \mathbf{u}_t d\Omega + \int_{\Omega} \mathbf{w} \nabla \cdot \mathbf{F}(\mathbf{u}) d\Omega + \int_{\Gamma} \mathbf{w} \mathbf{b}(\mathbf{u}, \mathbf{n}) d\Gamma = 0, \quad (35)$$

where again  $\mathbf{b}$  is a boundary operator, and  $\mathbf{n}$  is the normal vector at element interfaces. Application of the MZ-VMS procedure leads to

$$\int_{\Omega} \tilde{\mathbf{w}} \mathbf{u}_t d\Omega + \int_{\Omega} \tilde{\mathbf{w}} \nabla \cdot \mathbf{F}(\tilde{\mathbf{u}}) d\Omega + \int_{\Gamma} \tilde{\mathbf{w}} \mathbf{b}(\tilde{\mathbf{u}}, \mathbf{n}) d\Gamma = \tilde{\mathbf{M}} \int_0^t K(\tilde{\mathbf{a}}(t-s), s) ds. \quad (36)$$

The value of the memory at  $s = 0$  can be expressed as,

$$\tilde{\mathbf{M}}K(\tilde{\mathbf{a}}(t), 0) = \int_{\Omega} \tilde{\mathbf{w}} \nabla \cdot \mathbf{F}'(\mathbf{q}) d\Omega + \int_{\Gamma} \tilde{\mathbf{w}} \mathbf{b}'(\mathbf{q}, \mathbf{n}) d\Gamma, \quad (37)$$



where  $\mathbf{q}$  is given by,

$$\int_{\Omega} \mathbf{w}' \mathbf{q} d\Omega = \int_{\Omega} \mathbf{w}' \nabla \cdot \mathbf{F}(\tilde{\mathbf{u}}) d\Omega + \int_{\Gamma} \mathbf{w}' \mathbf{b}(\tilde{\mathbf{u}}, \mathbf{n}) d\Gamma. \quad (38)$$

The term  $\mathbf{F}' = \frac{\partial \mathbf{F}}{\partial \tilde{\mathbf{u}}}$  is the flux Jacobian and  $\mathbf{b}'$  is the numerical flux function linearized about  $\tilde{\mathbf{u}}$ . The resulting coarse-scale equation for the  $\tau$ -model is

$$\int_{\Omega} \tilde{\mathbf{w}} \mathbf{u}_t d\Omega + \int_{\Omega} \tilde{\mathbf{w}} \nabla \cdot (\mathbf{F}(\tilde{\mathbf{u}}) - \tau \mathbf{F}'(\mathbf{q})) d\Omega + \int_{\Gamma} \tilde{\mathbf{w}} (\mathbf{b}(\tilde{\mathbf{u}}, \mathbf{n}) - \tau \mathbf{b}'(\mathbf{q}, \mathbf{n})) d\Gamma = 0. \quad (39)$$

Consider now Eq. 34 augmented with an artificial viscosity term that is proportional to the orthogonal projection of the divergence of the flux,

$$\frac{\partial \mathbf{u}}{\partial t} + \nabla \cdot \mathbf{F} = \tau \nabla \cdot \mathbf{F}'(\Pi' \nabla \cdot \mathbf{F}). \quad (40)$$

A standard discretization technique for this second order equation is to split it into two first order equations<sup>1</sup>,

$$\frac{\partial \mathbf{u}}{\partial t} + \nabla \cdot (\mathbf{F}(\mathbf{u}) - \mathbf{F}'(\mathbf{q})) = 0, \quad (41)$$

with

$$\mathbf{q} = \Pi' \nabla \cdot \mathbf{F}(\mathbf{u}). \quad (42)$$

Assuming that the boundary operators are handled analogously, the discretization of Eq. 41 and Eq. 42 through finite elements leads to precisely Eqns. 38 and 39.

*Remarks*

1. For a hyperbolic conservation law, the memory is driven by a non-linear term that acts as a type of non-linear artificial viscosity.
2. The magnitude of the artificial dissipation is proportional to the projection of the flux onto the fine-scales. If the flux term is fully resolved, no information is added to the memory.
3. Due to the appearance of the orthogonal projector, it is difficult to comment on the sign of the artificial viscosity. While proofs exist showing that the term  $e^{t\mathcal{L}} \mathcal{P} \mathcal{L} \mathcal{Q} \mathcal{L} \tilde{\mathbf{a}}_0$  is globally dissipative in certain settings<sup>17</sup>, no such result is readily apparent in the general case.

## 6 Reduced Order Modeling

We extended the MZ- $\tau$  model to projection-based reduced order modeling in Ref. 22. The method is designed to be applied at the semi-discrete level and displays commonalities with the adjoint-stabilization method used in the finite element community as well as the least-squares Petrov-Galerkin<sup>4</sup> approach used in non-linear model order reduction. Theoretical error analysis shows conditions under which the new method, termed the Adjoint Petrov-Galerkin ROM, may have lower a priori error bounds than the Galerkin ROM. In the case of implicit time integration schemes, the Adjoint Petrov-Galerkin ROM was shown to be capable of being more efficient than least-squares Petrov-Galerkin when the non-linear system is solved via Jacobian-Free Newton-Krylov methods. Additionally, numerical evidence showed a correlation between the spectral

radius of the reduced Jacobian and the optimal value of the stabilization parameter appearing in the Adjoint Petrov-Galerkin method. When augmented with hyper-reduction, the Adjoint Petrov-Galerkin ROM was shown to be capable of producing accurate predictions within the POD training set with computational speedups up to 5000 times faster than the full-order models. This speed-up is a result of hyper-reduction of the right-hand side, as well as the ability to use explicit time integration schemes at large time-steps. A study of the Pareto front for simulation error versus relative wall time showed that, for the compressible cylinder problem, the Adjoint Petrov-Galerkin ROM is competitive with the Galerkin ROM. Both the Galerkin and Adjoint Petrov-Galerkin ROM were more efficient than the LSPG ROM for the problems considered.

## 7 Entropy Conservative and Stable Formulations

Non-linear stability is a desirable, but elusive topic in the analysis of numerical methods for complex PDEs. There are many notions of non-linear stability, but we will consider Entropy stability in the sense of Tadmor<sup>23</sup>.

A number of systems of conservation laws imply additional conservation equations for mathematical entropies, namely scalar convex functions of the conserved variables. For instance, the compressible one dimensional Euler equations imply:

$$\frac{\partial(-\rho s)}{\partial t} + \frac{\partial(-\rho u s)}{\partial x} = 0,$$

where  $s = \ln(p)\gamma\ln(\rho)$  is the specific entropy. In shock calculations, another well-established guideline is that entropy should be produced across shocks. In more formal terms, this is equivalent to requiring that the numerical scheme should be consistent with the inequality:

$$\frac{\partial(-\rho s)}{\partial t} + \frac{\partial(-\rho u s)}{\partial x} \leq 0$$

Building from extensive theoretical work on the structure of such systems, Tadmor<sup>23</sup> introduced discretizations which are consistent with either the conservation equation for entropy or the entropy inequality at the semi-discrete level. The scheme is termed Entropy-Conservative (EC) in the first case and Entropy-Stable (ES) in the second case.

## 8 Non-linear Stability of MZ- $\tau$ models

We will now consider the stability of the MZ- $\tau$  models. The starting point (i.e. the fully resolved numerics) should be Entropy conservative. Consider the governing equations in weighted residual form,

$$(\mathbf{w}, \mathbf{u}_t) + (\mathbf{w}, \mathcal{R}(\mathbf{u})) = 0. \tag{43}$$

For simplicity, the following derivation will neglect boundary operators. To derive an evolution equation for entropy, first set  $\mathbf{w} = \mathbf{v}^T$ ,

$$(\mathbf{v}^T, \mathbf{u}_t) = -(\mathbf{v}^T, \mathcal{R}(\mathbf{u})) = 0. \tag{44}$$

Note that it is only possible to set  $\mathbf{w} = \mathbf{v}^T$  for formulations where  $\mathbf{v}$  is in the subspace spanned by the basis functions. This is the case when one discretizes in entropy variables, but not when one discretizes in conservative variables. Proceed by splitting  $\mathbf{v}$  into coarse and fine scales,

$$(\tilde{\mathbf{v}}^T, \mathcal{R}(\mathbf{u}(\tilde{\mathbf{v}} + \mathbf{v}')))) + (\mathbf{v}'^T, \mathcal{R}(\mathbf{u}(\tilde{\mathbf{v}} + \mathbf{v}')))) = 0. \quad (45)$$

Setting  $\mathbf{v}' = 0$ , it is seen that,

$$(\tilde{\mathbf{v}}^T, \mathcal{R}(\mathbf{u}(\tilde{\mathbf{v}}))) = 0. \quad (46)$$

Now set  $\mathbf{v}' = \epsilon \mathbf{h}$ ,

$$(\tilde{\mathbf{v}}^T, \mathcal{R}(\mathbf{u}(\tilde{\mathbf{v}} + \epsilon \mathbf{h}))) + (\epsilon \mathbf{h}^T, \mathcal{R}(\mathbf{u}(\tilde{\mathbf{v}} + \epsilon \mathbf{h}))) = 0. \quad (47)$$

Expanding in a Taylor series and using the chain rule,

$$(\tilde{\mathbf{v}}^T, \mathcal{R}(\mathbf{u}(\tilde{\mathbf{v}}))) + \epsilon (\mathbf{h}^T, \mathcal{R}(\mathbf{u}(\tilde{\mathbf{v}}))) + (\tilde{\mathbf{v}}^T, \frac{\partial \mathcal{R}}{\partial \mathbf{u}} \frac{\partial \mathbf{u}}{\partial \mathbf{v}} \epsilon \mathbf{h})) + \epsilon^2 (\mathbf{h}^T, \frac{\partial \mathcal{R}}{\partial \mathbf{u}} \frac{\partial \mathbf{u}}{\partial \mathbf{v}} \epsilon \mathbf{h}) = 0. \quad (48)$$

Setting,

$$\mathbf{h} = \Pi'_{\mathbf{v}} \mathcal{R}(\mathbf{u}(\tilde{\mathbf{v}})),$$

where  $\Pi'_{\mathbf{v}}$  is the projection onto the fine scales (i.e. the fine-scale mass matrix) as defined by the entropy variables,

$$\Pi'_{\mathbf{v}} f = \mathbf{w}'^T \left[ \int \mathbf{w}' \frac{\partial \mathbf{u}}{\partial \mathbf{v}} \mathbf{w}'^T d\Omega \right]^{-1} (\mathbf{w}', f). \quad (49)$$

The entropy evolution for the  $\tau$  and VMS( $\epsilon$ ) models is given by,

$$\left( \tilde{\mathbf{v}}^T, \frac{\partial}{\partial t} \mathbf{u}(\tilde{\mathbf{v}}) \right) + \left( \tilde{\mathbf{v}}^T, \mathcal{R}(\mathbf{u}(\tilde{\mathbf{v}})) \right) + \left( \tilde{\mathbf{v}}^T, \tau \frac{\partial \mathcal{R}}{\partial \mathbf{u}} \frac{\partial \mathbf{u}}{\partial \mathbf{v}} \Pi'_{\mathbf{v}} \mathcal{R}(\mathbf{u}(\tilde{\mathbf{v}})) \right) \leq 0 \quad \forall \tau > 0. \quad (50)$$

It is seen that, in an entropy conservative formulation, the  $t$ ,  $\tau$ , and VMS( $\epsilon$ ) models dissipate entropy. Hence, the schemes are entropy stable.

## 8.1 Example

As an example, if one begins with an an entropy conservative flux<sup>18</sup> for the Burgers equation,

$$\hat{F}(u_R, u_L) = \frac{1}{6} (u_R^2 + u_L u_R + u_L^2), \quad (51)$$

application of the MZ- $\tau$  leads to the corresponding flux function is

$$f(u_R, u_L) = \frac{1}{6} (u_L^2 + u_L u_R + u_R^2) - \frac{\tau}{18} (5u_L^2 + 8u_L u_R + 5u_R^2). \quad (52)$$

For all  $\tau > 0$ , the above is an entropy stable flux function. The choice of  $\tau$  controls the amount of dissipation added to the system.

For an initial condition  $u(x, 0) = \sin(x)$ , Figure 4 shows results of Discontinuous Galerkin simulations using one element and a third order polynomial (four total DOFs). The results are compared to a projected solution that was obtained using  $p = 127$ . In Figure 4, one can see that simulations run using an entropy conservative flux and central flux under-predict the dissipation in resolved entropy. The entropy conservative flux leads to no net decrease in entropy, while the

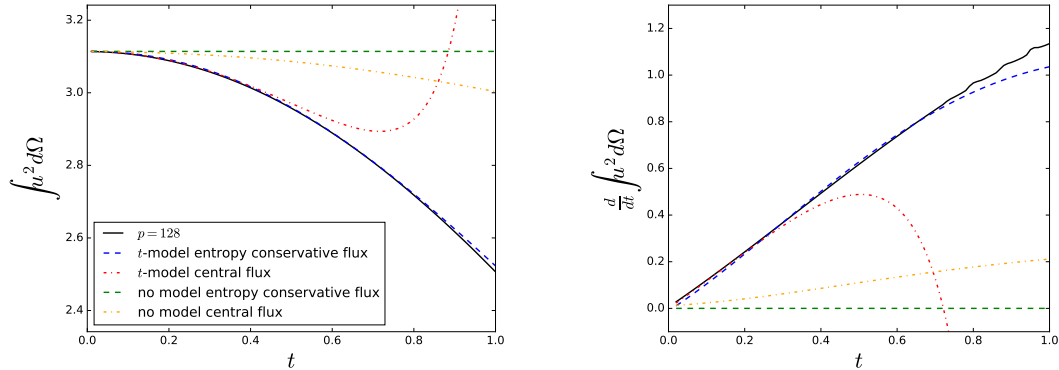


Figure 4: Numerical solutions to the Burgers' equation using 1 element with  $p = 3$ .

central flux leads to a slight decrease in entropy. The results of the Roe scheme are not shown in Figure 4 as they are comparable to the central flux. Figure 4 shows the importance of the flux function for the MZ-VMS models. It is seen that the  $t$ -model constructed from the central flux rapidly goes unstable. This instability is not surprising since the central flux does not guarantee entropy conservation and hence it is possible for the MZ-VMS model to add entropy to the system. The  $t$ -model constructed from an entropy conservative flux provides a stable and accurate solution.

## 9 Contributions to Entropy stable methods

Having recognized that Entropy conservative formulations offer a route to provable non-linear stability of MZ formulations, we made several advances to the theory of EC/ES methods. The following is a summary:

A key question in the use of ES methods is how much entropy should be produced by the scheme at a certain level of under-resolution. This problem has been so far studied by considering different ES interface fluxes in the spatial discretization, only because they can be tuned to generate a certain amount of entropy. In Ref. 12 note, we point out that, in the context of space-time discretizations, the same applies to ES interface fluxes in the temporal direction.

The current state-of-the-art solves the compressible Navier-Stokes equations for a single-component perfect gas in chemical and thermal equilibrium. As a first step towards enabling the use of EC/ES schemes in complex applications such as Hypersonics and Combustion, we formulated ES schemes for the multicomponent compressible Euler equations in Ref. 13. Special care had to be taken as we discovered that the theoretical foundations of ES schemes begin to crumble in the limit of vanishing partial densities.

The realization that ES schemes can only go as far as their theory led us to review some of it. A fundamental result supporting the development of limiting strategies for high-order methods is the minimum entropy principle proved by Tadmor for the compressible Euler equations. It states that the specific entropy of the physically relevant weak solution does not decrease. In Ref. 14, we prove a minimum entropy principle for the mixtures specific entropy in the multicomponent

case, which implies that the aforementioned limiting strategies could be extended to this system.

In Ref. 11 (two journal submissions are upcoming on this topic), we study the behavior of ES schemes in the low Mach number regime, where shock-capturing schemes are known to suffer from severe accuracy degradation issues. A classic remedy to this problem is the flux-preconditioning technique, which consists in tweaking artificial dissipation terms to enforce consistent low Mach behavior. We showed that ES schemes suffer from the same issues and that the flux-preconditioning technique can improve their behavior without interfering with entropy-stability. Furthermore, we demonstrated analytically that these issues stem from an acoustic entropy production field which scales improperly with the Mach number, generating spatial fluctuations that are inconsistent with the equations. An important outgrowth of this effort is the discovery that skew-symmetric dissipation operators can alter the way entropy is produced locally, without changing the total amount of entropy produced.

## References

- [1] F. Bassi and S. Rebay. A high order accurate discontinuous finite element method for the numerical solution of the compressible navier-stokes equations. *Journal of Computational Physics*, 131:267–279, 1997.
- [2] Camilo Bayona, Joan Baiges, and Ramon Codina. Variational multi-scale approximation of the one-dimensional forced burgers equation: the role of orthogonal sub-grid scales in turbulence modeling. *International Journal for Numerical Methods in Fluids*, 2017.
- [3] David Bernstein. Optimal prediction of burgers’s equation. *Multiscale Model. Simul.*, 6(1):27–52, 2007.
- [4] Kevin Carlberg, Matthew Barone, and Harbir Antil. Galerkin v. least-squares petrov-galerkin projection in nonlinear model reduction. *Journal of Computational Physics*, 330:693–734, 2017.
- [5] Alexandre J. Chorin, O. Hald, and R. Kupferman. Optimal prediction and the mori-zwanzig representation of irreversible processes. *Proc. Natl Acad. Sci.*, 97((doi:10.1073/pnas.97.7.2968)):2968–2973, 2000.
- [6] Alexandre J. Chorin and Ole H. Hald. *Stochastic Tools for Mathematics and Science*. Springer, 2013.
- [7] Alexandre J. Chorin, Ole H. Hald, and Raz Kupferman. Prediction from partial data, renormalization, and averaging. *Journal of Scientific Computing*, 28(2-3):245–261, September 2006.
- [8] Ramon Codina. Stabilization of incompressibility and convection through orthogonal subscales in finite element methods. *Computer methods in applied mechanics and engineering*, 190(1579-1599), 2000.
- [9] Ramon Codina. Stabilized finite element approximation of transient incompressible flows using orthogonal subscales. *Computer methods in applied mechanics and engineering*, 191(4295-4321), 2002.

- [10] Dror Givon, Ole H. Hald, and Raz Kupferman. Existence proof for orthogonal dynamics and the mori-zwanzig formalism. *Israel Journal of Mathematics*, 145(1):221–241, 2005.
- [11] Ayoub Gouasmi. *Contributions to the Development of Entropy-Stable Schemes for Compressible Flows*. PhD thesis, University of Michigan, 2019.
- [12] Ayoub Gouasmi, Karthik Duraisamy, and Scott Murman. On entropy stable temporal fluxes. *arXiv preprint arXiv:1807.03483*, 2018.
- [13] Ayoub Gouasmi, Karthik Duraisamy, and Scott Murman. Formulation of entropy-stable schemes for the multicomponent compressible euler equations. *arXiv preprint arXiv:1904.00972*, 2019.
- [14] Ayoub Gouasmi, Karthik Duraisamy, Scott M Murman, and Eitan Tadmor. A minimum entropy principle in the compressible multicomponent euler equations. *ESAIM: Mathematical Modeling and Numerical Analysis*, 2019.
- [15] Ayoub Gouasmi, Eric J. Parish, and Karthik Duraisamy. A priori estimation of memory effects in reduced-order models of nonlinear systems using the mori-zwanzig formalism. *Proceedings of The Royal Society A*, 473(20170385), 2017.
- [16] Oriol Guasch and Ramon Codina. Statistical behavior of the orthogonal subgrid scale stabilization terms in the finite element large eddy simulation of turbulent flows. *Computer methods in applied mechanics and engineering*, 261-262(154-166), 2013.
- [17] Ole H. Hald and P. Stinis. Optimal prediction and the rate of decay for solutions of the euler equations in two and three dimensions. *Proceedings of the National Academy of Sciences*, 2007.
- [18] Farzad Ismail. *TOWARD A RELIABLE PREDICTION OF SHOCKS IN HYPERSONIC FLOW: RESOLVING CARBUNCLES WITH ENTROPY AND VORTICITY CONTROL*. PhD thesis, University of Michigan, 2006.
- [19] B.O. Koopman. Hamiltonian systems and transformations in hilbert space. *Proceedings of the National Academy of Sciences of the US A*, 17(5):315–318, 1931.
- [20] Eric J. Parish and Karthik Duraisamy. A dynamic subgrid scale model for large eddy simulations based on the mori-zwanzig formalism. *Journal of Computational Physics*, 349(15):154–175, 2017.
- [21] Eric J Parish and Karthik Duraisamy. A unified framework for multiscale modeling using the mori-zwanzig formalism and the variational multiscale method. *arXiv preprint arXiv:1712.09669*, 2017.
- [22] Eric J Parish, Christopher Wentland, and Karthik Duraisamy. The adjoint petrov-galerkin method for non-linear model reduction. *arXiv preprint arXiv:1810.03455*, 2018.
- [23] Eitan Tadmor. Entropy stability theory for difference approximations of nonlinear conservation laws and related time-dependent problems. *Acta Numerica*, 12:451–512, 2003.